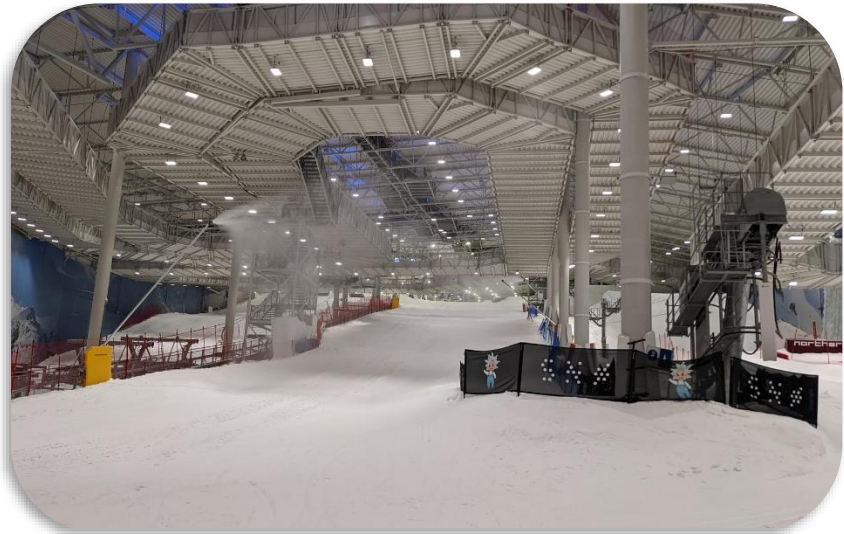


Susanne Lang

***Indoor refrigeration system for snow
production – design and optimization***

*Innendørs kundesystem for snøproduksjon
– utforming og optimering*

Desember 2021



PROJECT WORK

for

student Susanne Lang

Fall 2021

Indoor refrigeration system for snow production – design and optimization *Innendørs kundesystem for snøproduksjon – utforming og optimering*

Background and objective

The project, “Snow for the Future”, is in cooperation with FIS, NSF, Trondheim community and with NTNU and SINTEF as operation partners. One of the tasks is to investigate indoor snow production and improvement of the current systems. The reference system will be the “SNØ” facilities close to Oslo. In this facility the snow is produced with traditional snow cannons and lances in the total hall. The temperature in the hall must be low enough (-8 - -10°C) to be able to produce snow in the open volume.

The project work will investigate the system to make a snow producing towers, placed in strategic point, and let the temperature in the hall be raised to a temperature below the freezing point and only have low temperature for snow production in the towers. This will reduce the energy consumption of the hall. Total energy analysis, refrigeration system and defrosting of evaporators will be investigated.

The following tasks are to be considered:

1. Literature review of indoor snow production
2. Make model for calculation of the energy consumption of the hall at different indoor temperatures
3. Investigation of the snow production system, operation, and energy consumption of the systems
4. Compare the system with production in hall and with the snow producing towers
5. Investigate the alternative defrosting systems for the evaporators.
6. Make proposal for further work

-- “ --

The project work comprises 15 ECTS credits.

The work shall be edited as a scientific report, including a table of contents, a summary in Norwegian, conclusion, an index of literature etc. When writing the report, the candidate must emphasise a clearly arranged and well-written text. To facilitate the reading of the report, it is important that references for corresponding text, tables and figures are clearly stated both places. By the evaluation of the work the following will be greatly emphasised: The results should be thoroughly treated, presented in clearly arranged tables and/or graphics and discussed in detail.

The candidate is responsible for keeping contact with the subject teacher and teaching supervisors.

Risk assessment of the candidate's work shall be carried out according to the department's procedures. The risk assessment must be documented and included as part of the final report. Events related to the candidate's work adversely affecting the health, safety or security, must be documented and included as part of the final report. If the documentation on risk assessment represents a large number of pages, the full version is to be submitted electronically to the supervisor and an excerpt is included in the report.

According to "Utfyllende regler til studieforskriften for teknologistudiet/sivilingeniørstudiet ved NTNU" § 20, the Department of Energy and Process Engineering reserves all rights to use the results and data for lectures, research and future publications.

Submission deadline: December 17th

- ☐ Work to be done in lab (Water power lab, Fluids engineering lab, Thermal engineering lab)
☐ Field work

Department for Energy and Process Engineering, *August 2021*



Prof. Trygve M. Eikevik
Supervisor

Co-Supervisor(s):

Abstract

The objective of this thesis is to improve the energy efficiency of indoor ski facilities. The reference indoor ski hall is "SNØ", which is located near Oslo. In order to achieve good snow quality, the temperature in the ski hall must be lowered for the snow production. To reduce the energy consumption, a snow production system was designed and evaluated in which snow is produced in external snow production towers. The basic idea of the external snow production towers is to keep the temperature of the hall constant without the need for cooling down the complete hall for the snow production. The evaluation of the energy efficiency showed that 44 928 kWh of electricity can be saved per year if the external snow production towers are used compared to the snow production in the hall. These 44 928 kWh correspond to about 0.7 % of the total energy consumption of the indoor ski hall.

Contents

Abstract	I
Contents.....	II
List of Figures	IV
List of Tables.....	V
Nomenclature	VI
1 Introduction.....	5
1.1 Background	5
1.2 Objectives.....	5
1.3 Outline of thesis	5
2 Indoor snow production	6
2.1 Production of artificial snow	6
2.1.1 Key conditions.....	8
2.1.2 Characteristics of artificial snow	8
2.2 Temperature dependent snowmaking machines	9
2.3 Literature review on indoor ski facilities	11
3 Design of the production towers	16
3.1 Calculation of the droplet freezing time.....	17
3.2 Humidity in the production towers.....	19
4 Energy analysis	23
5 Defrosting systems for evaporators.....	30
6 Conclusions and suggestions for further work.....	33
6.1 Conclusion.....	33
6.2 Suggestions for further work.....	33
7 References.....	34
Appendix	A

List of Figures

Figure 1: Freezing stages of a droplet. (Akhtar et al. 2020).....	7
Figure 2: Production of artificial snow with a snow canon. (Singh and Singh 2011)	7
Figure 3: Snow quality chart depending on the wet bulb temperature. (Trædal 2017).....	8
Figure 4: Crystal shape of artificial snow. (Singh and Singh 2011)	9
Figure 5: D800+ snow gun. (Cardillo et al. 2015)	10
Figure 6: Atomizers and nucleators fitted at the outlet of the fan. (Cardillo et al. 2015)	10
Figure 7: Snow lance. (Eurrer 2021).....	10
Figure 8: Snow production tower Skidome Prioritet Serene Arena. (Fredheim 2019).....	13
Figure 9: Sketch of the hall with the external snow production towers (red)	16
Figure 10: Sketch of production tower with air flow	17
Figure 11: Freezing time as a function of the air temperature	18
Figure 12: Typical droplet size distribution. (Liao and C. 1989).....	19
Figure 13: Additional energy needed compared to an indoor temperature of - 5 °C with lower temperature. Considering additional transmission losses for an average outdoor temperature of 8.3 °C. E_{cool} for starting temperature of - 5 °C.	24
Figure 14: Energy demand ($Q_{cool}+Q_{trans}$) for an indoor temperature of -10 °C.....	25
Figure 15: Refrigeration system.....	25
Figure 16: Pressure-Enthalpy diagram CO_2	29
Figure 17: Schematic of hot gas bypass defrosting of an transcritical CO_2 heat pump. (Wang et al. 2020).....	32

List of Tables

Table 1: Characteristics of artificial snow compared to natural snow (Singh and Singh 2011)	9
Table 2: Examples of indoor snow centers	14
Table 3: Parameter freezing time calculation.....	18
Table 4: Thermal properties	20
Table 5: Cooling demands.....	27
Table 6: Results calculation refrigeration system	28
Table 7: Thermal properties water (Akhtar et al. 2020).....	A
Table 8: Specific heat capacities dry air and vapor (Doering et al. 2016)	A
Table 9: Refrigeration system hall (pressure, enthalpy)	A
Table 10: Refrigeration system towers.....	A

Nomenclature

A	Area	m ²
c _p	Specific heat capacity	J/(kgK)
D	Diffusion coefficient	m ² /s
d	Diameter	
h	Enthalpy	kJ/kg
k _A	Mass transfer coefficient	m/s
M	Molar mass	kg/mol
\dot{m}	Mass flow	kg/s
p	Vapor pressure	Pa
Q	Heat	kW
R	Universal gas constant	(kg m ²)/(s ² molK)
T	Temperature	°C/K
t	Time	s
U	Overall heat transfer coefficient	W/(m ² K)
V	Volume	m ³
W	Work	kW
η	Dynamic viscosity air	kg/(m · s)
ν	Kinematic viscosity	kg/(m · s)
ρ	Density	kg/m ³
φ	Relative humidity	%
Re	Reynolds number	
Sc	Schmidt number	
Sh	Sherwood number	

Abbreviations

VTT	Technical Research Centre of Finland
HTC	Heat transfer coefficient
COP	Coefficient of performance

1 Introduction

1.1 Background

The first indoor ski facility was built in Adelaid, Australia in 1982. Since then, indoor ski facilities got more and more popular. In 2019, there were about 50 year-round indoor ski facilities worldwide. (Skoblickaya and Sherement 2019)

This thesis is part of the project “snow for the future” which objective is to develop climate-friendly and cost-effective technologies for artificial snow production. To achieve a good snow quality the temperature of the indoor ski hall needs to be lowered during the time of snow production. Cooling the indoor ski hall down for snow production accounts for a not insignificant share of the energy consumption. If the snow is produced outside the main ski hall, there is no need to cool the entire hall.

1.2 Objectives

The objective of this thesis is to investigate indoor snow production systems and to develop a new system in which the snow is generated outside the ski hall. The reference system is "SNØ" which is located near Oslo. For this reference system, external production towers should be designed and the energy efficiency should be evaluated. Then, the new system should be compared with the current system, especially in terms of the energy efficiency. Alternative defrosting systems for the evaporators should also be investigated.

1.3 Outline of thesis

After the introduction, a literature study about artificial snow production will follow. The second part of the literature study is about indoor ski facilities in particular. Chapter 3 presents the new snow production system and the comparison with the current system regarding the energy consumption. In chapter 5 an overview of defrosting systems for the evaporators is given, followed by the conclusion and suggestions for further work.

2 Indoor snow production

2.1 Production of artificial snow

The formation of natural snow starts with the growth of an ice crystal around a cloud condensation nuclei. The ice crystal grows by the further deposition of water vapor. The ice crystals can aggregate and form a bigger snow flake. (Singh and Singh 2011)

The formation of artificial snow is different to those of natural snow. Artificial snowmaking can be divided into temperature-independent and temperature-dependent processes. Temperature-dependent processes, e.g. flake ice makers, tube ice makers, plate ice makers or ice slurry machines produce small ice grains. But for this thesis the process of interest is the temperature-dependent process, which will be described in more detail in the following part.

A temperature dependent way to produce artificial snow is to atomize water, which then freezes at low temperatures. The following describes the process, how artificial snow is formed. Compressed water, which is just above the freezing point is ejected through a nozzle. When the water is premixed with air, the nozzle is called nucleator. When only water is ejected, it is called atomizer. (A. Koptug, J. Aström, L. Ananiev 2006) Due to the expansion, the temperature of the air drops. Convective heat transfer lowers the temperature of the droplet. Further cooling effect is due to evaporation from the drop surface. It cools the drop down to the wet-bulb temperature of the air (Olefs et al. 2009). Assuming a drop size of 600 μm and a terminal falling velocity of 2.5 m/s, the heat transfer due to the evaporation is predominant with temperatures above $-7\text{ }^{\circ}\text{C}$. At lower temperatures the convective heat transfer predominates. (Chen and Kevorkian 1971)

These cooling effects lead to the subcooling of the droplet, which is the first stage of the freezing process, see Figure 1: Freezing stages of a droplet. (Akhtar et al. 2020) In this area the atomization of the water droplets takes place. This reduces the drop size to about 200 μm to 300 μm . The smaller the drop is the better the heat transfer rate is, because the area-unit mass ratio is higher. After the atomization, i.e. in the range of 50 cm to 100 cm after the ejection, nucleation is the dominant process, see Figure 2. Thereby the water droplets freeze to ice particles with a size of about 50 μm . (Singh and Singh 2011) When the drop is subcooled, impurities can initiate the heterogenous nucleation. Without the impurities or an external contact water can stay liquid down to $-40\text{ }^{\circ}\text{C}$ (Liao and C. 1989). The freezing process

continues with dendritic growth, increasing in temperature until equilibrium solidification. When the water is completely frozen the temperature of the drop is decreasing again, see Figure 1. (Akhtar et al. 2020).

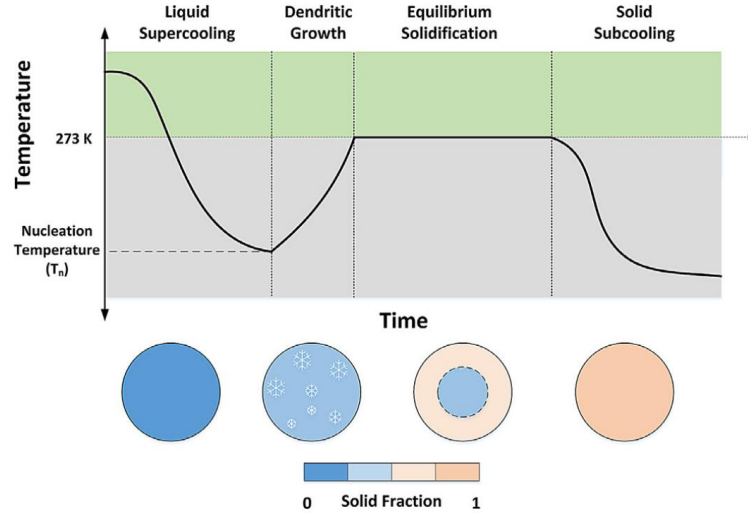


Figure 1: Freezing stages of a droplet. (Akhtar et al. 2020)

The resulting ice crystal grows by the condensation of water vapor on its surface. This process, which is prevalent in the range of 200 cm to 500 cm after the ejection, is called seeding. Further growth is due to evaporation of water that adheres to the ice crystal and the cooling that accompanies it. The evaporation is followed by convection, which occurs about 1 m to 80 m from the snow gun. (Singh and Singh 2011)

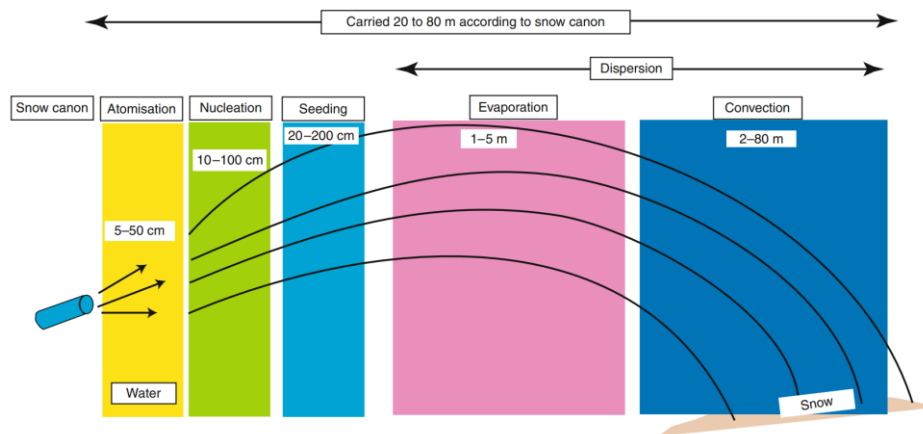


Figure 2: Production of artificial snow with a snow canon. (Singh and Singh 2011)

A lot of research has been done on the complex process of freezing of a falling droplet in recent years. A good overview of the research on this topic is given in (Xin Zhao, Bo Dong, Weizhong Li 2018). Theoretical, experimental and numerical approaches are briefly described. The newest

study found (El Achkar 2019) is using a numerical model to investigate the effects of the air temperature, relative humidity and velocity, the initial droplet diameter and initial temperature.

2.1.1 Key conditions

As mentioned earlier, the presence of impurities, droplet size, and droplet velocity, which affect heat transfer, are parameters that influence the freezing process. The key parameter is the wet-bulb temperature. It combines the dry-bulb temperature (air temperature measured with a thermometer) and the relative humidity. The cooling effect due to the evaporation from the droplet surface cools the droplet down to the wet-bulb temperature of the air. At a lower air humidity, more water evaporates from the surface, resulting in a stronger cooling effect. (Olefs et al. 2009) The chart in Figure 3 shows the wet-bulb temperature required for good snow quality depending on the dry-bulb temperature and the relative humidity. Producing snow in a smaller space causes the humidity to rise higher, which requires a lower air temperature to maintain the same wet-bulb temperature. This is an issue that must be addressed in the design of the external snow producing towers.



Figure 3: Snow quality chart depending on the wet bulb temperature. (Trædal 2017)

2.1.2 Characteristics of artificial snow

The different formation process of artificial snow leads to different characteristics compared to natural snow. Artificial snow, for example, does not have the typical dendritic shape, but a spherical one, as shown in Figure 4.

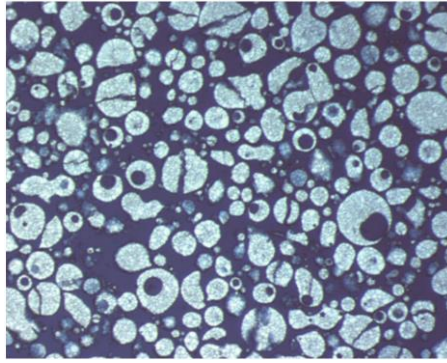


Figure 4: Crystal shape of artificial snow. (Singh and Singh 2011)

Not only the shape is different, but also other properties such as grain size, density and conductivity differ. The density is about 4 times higher compared to natural snow, see Table 1. (Singh and Singh 2011)

Table 1: Characteristics of artificial snow compared to natural snow (Singh and Singh 2011)

	Artificial snow	Natural snow
Grain size	0.05 to 2 mm	0.2 to several mm
Shape	Small round particles, spherical, may contain air pocket	Dendritic
Density	300 to 500 kg/m ³	4 times lower
Conductivity	> 85 μ S/cm	10 times lower

2.2 Temperature dependent snowmaking machines

Fan guns and lances are the most common technologies to produce artificial snow.

Fan gun

A fan gun consists of a jet fan for the air supply and nozzles, which eject pressurized water into the jet. The main components are an air compressor, a fan with its driving motor, nozzle rings, nucleator ring and electrical resistance to prevent ice formation inside the nozzle system. The water mass flow and thus the production capacity can be regulated. An example of a snow gun is illustrated in Figure 5. The nozzle system, which is fitted at the outlet of the fan is shown in Figure 6. (Cardillo et al. 2015)

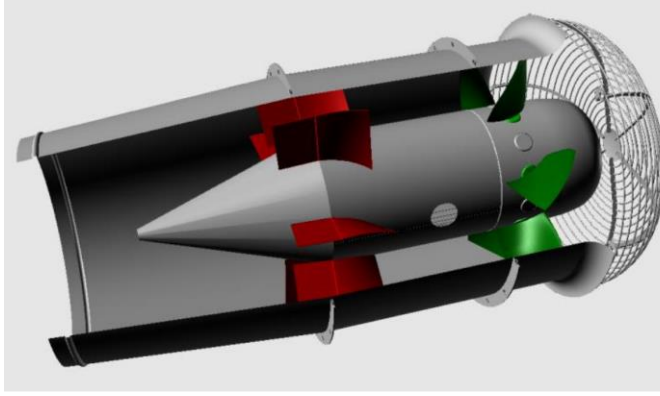


Figure 5: D800+ snow gun. (Cardillo et al. 2015)

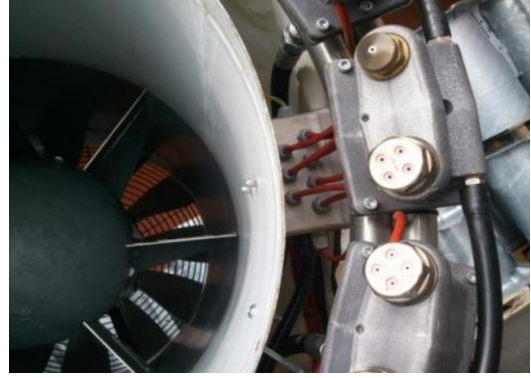


Figure 6: Atomizers and nucleators fitted at the outlet of the fan. (Cardillo et al. 2015)

Techno Alpin developed a fan gun especially for indoor conditions. According to the manufacturer it has the following advantages. The system can operate with temperatures up to $-2\text{ }^{\circ}\text{C}$ and is independent of the humidity. Unlike conventional fan guns, it has an integrated heat exchanger, which allows the system to cool the air mass flow itself. It also has a lower influence on the temperature and the air humidity of the hall. (Techno Alpin 2021)

Lances

Lances use high-pressure water and high-pressure air. Due to the expansion the water cools down. To ensure that the droplet has enough time to freeze till it falls on the ground, the lances are up to 10 m high. (Arnold Ofner 2006) An advantage of the snow lances are the lower energy consumption and a lower noise level when they are compared with fan guns. A disadvantage is the lower production rate. (Vagle 2016)



Figure 7: Snow lance. (Eurrer 2021)

2.3 Literature review on indoor ski facilities

Although the number of indoor ski halls is steadily increasing and artificial snow is also being used more and more frequently, scientific literature is still limited. Google Scholar and Oria, the NTNU Library's literature search tool, were used for the literature search. The work of (Fanasiutkia 2015) and (Fredheim 2019) are mainly concerned with the energy consumption and how to optimize it. (Sipilä and Rämä 2009) also evaluated the energy consumption of a ski tunnel. It is the only work found in which the cooling system is described more detailed. In the thesis of (Fröjd 2014) different ways to produce the snow are analyzed, with regard to the energy efficiency.

The organization of air exchange of ski tunnel - Lappeenranta

In this bachelor thesis of the Saimaa University of Applied Sciences, Lappeenranta, an air exchange system for the ski tunnel in Khanty-Mansiysk, Russia was analyzed. A detailed thermal calculation and a calculation of the air parameters were performed. This analysis showed that the thermal properties of the walls should be improved to reduce the energy consumption. In addition, the air flow in the tunnel was analyzed with a numerical simulation, to design an air exchange system. (Fanasiutkia 2015)

Energy systems for an artificial cross-country skiing tunnel – Chalmers university – Gothenburg

(Fredheim 2019) investigated the energy systems of various cross-country ski tunnels in her master's thesis, focusing on snow quality. Therefore, three different ski tunnels were described and analyzed. The evaluation showed that air leakages contributed to a large extent to the energy losses. The three described ski tunnels are located in Torsby, Gällö and Gothenburg, Sweden. Additional information about these are given in Table 2. (Fredheim 2019)

Integrated heating and cooling technology for sport facilities– VTT research center Finland

The main topic of this publication from the Technical Research Centre of Finland (VTT) is the integrated heating and cooling of sports facilities. The study subject is the Vatherus skiing ring in Uusikaupunki, Finland, see Table 2. The surplus heat is used in to heat the adjacent sport facilities. The design cooling capacity is 400 kW, 350 kW for the air cooling and 50 kW for the ground cooling. To evaluate the energy consumption a Simulation tool was used, which modeled the production and the consumption of the heating and cooling. In addition to this the use of CO₂ as a heat transfer medium was studied. A CO₂-piping was designed based on

measured data of the skiing ring. The evaluation of the CO₂-piping concludes that CO₂ is well suited in this application. (Sipilä and Rämä 2009)

Energy efficient production and storage of snow for snow tunnel – Luleå

In the thesis of (Fröjd 2014) different ways to produce snow for a ski tunnel and the storage of it were analyzed. The study subject is the ski tunnel at Lindbäcksstadion close to Piteå, Sweden. The four ways are: storing natural snow, produce artificial snow outside, produce the snow inside the ski tunnel or use an external production site. These methods have been compared regarding energy consumption, the cost and the operation-related environmental impact. A hall with dimensions of 60 x 35 m and a height of 8 m was considered as an external production site. The snow should be produced with a snow canon in this external hall. The calculation of the energy consumption showed a 21 % lower energy consumption for the production in this external hall compared to the production in the ski tunnel. (Fröjd 2014)

Examples indoor ski facilities




Table 2 shows the results of the literature review on indoor ski facilities for which basic data are available. All the indoor ski facilities are for cross-country skiing. No indoor ski facility with an alpine slope were found for which there were data on energy consumption or snow production. The snow for the ski halls in Torsby and Gällö is produced with snow cannons outside the halls during the winter. For the indoor ski hall in Gothenburg the snow is produced in a external snow tower, see Figure 8. (Fredheim 2019).





Figure 8: Snow production tower Skidome Prioritet Serene Arena. (Fredheim 2019)

In (Fröjd 2014) the energy consumption per square meter and year is given for the indoor ski tunnels in Uusikaupunki, Vaukatti and Leppävirta. The energy consumption is between 44 kWh/(m² year) to 73 kWh/(m² year). "SNØ" has an area of 32 000 m² and an energy consumption of 6 000 000 kwh per year (Klingenberg 2021). On this basis, on the energy consumption of 13 kWh/(m² year) is significantly lower compared to the other halls.

Table 2: Examples of indoor snow centers

	Location / year	Description	Temperature	Additional information	References
	Torby skidtunnel Torsby, Sweden 2006	Track: 1.3 km Tunnel out of concrete, covered by soil for insulation	-3 to 0°C	<ul style="list-style-type: none"> Artificial snow produced outside and exchanged once a year. 8 stand-alone ventilation systems with heat exchangers 	(Fredheim 2019)
	MidSweden365 Gällö, Sweden 2017	Track: 1.4 km	-4°C	<ul style="list-style-type: none"> Snow produced outside Most of the parts of the tunnel are in a mountain CO2 sensors monitor air quality so that air is exchanged only when necessary Snow volume 4 000m³ Floor insulation: coils for cooling in a frozen water-sand bed 	(MidSweden365 2021; Fredheim 2019)
	Skidome Prioritet Serene Arena Gothenburg, Sweden 2015	Track: 1.2 km	-3 to -4	<ul style="list-style-type: none"> Snow production outside the building. Snow is changed once a year. 	(Fredheim 2019; Website Skidome Göteborg 2021; Afry 2021)

	Vahterusring Finland (Uusikaupunki) 2005	Track: 1 km Area 5 000 m ²	-1.7°C (air temperature)	<ul style="list-style-type: none"> Energy consumption: 73 kWh/ (year m²), using CO₂ as a refrigerant. 	(Fröjd 2014; Sipilä and Rämä 2009)
	Vuokatti Ski Tunnel Finland (Voukatti) 1998	Area: 9 600 m ²	-5 to -9	<ul style="list-style-type: none"> Energy consumption: 63 kWh/(year m²) 	(Fröjd 2014; Website Vuokatti 2021)
	Vesileppis Skiing Arena Finland (Leppävirta) 2004	Area: 8 000 m ² Volume: 55 000 m ³	-1 to -5 °C Humidity 75%	<ul style="list-style-type: none"> Energy consumption: 44 kWh/(year m²) 	(Fröjd 2014; Website Vesileppis)
	LOTTO Thüringen Skisport-HALLE Germany (Oberhof) 2009	Area: 1 100 m ²	-3 to -4 (air temperature) -5 to -7 (snow temperature) Humidity 80 to 100 %		(Website Skihall Oberhof 2021; Website Thüringer Wintersportzentrum 2021)

3 Design of the production towers

The reference indoor ski hall “SNØ” was completed in early 2020. It is located in Lørenskog, about 15 km northeast from the center of Oslo. “SNØ” has a 500 m alpine slope and a 1.5 km cross-country track. Next to the ski hall restaurants, shops and hotels are located that use the surplus heat from the refrigeration system. During snow production, the temperature in the hall is lowered from $-5\text{ }^{\circ}\text{C}$ to $-7/-10\text{ }^{\circ}\text{C}$. Snow production takes place once a week from Sunday 6 pm to Monday 3 pm.

To reduce the energy consumption, the objective of this work is to investigate a new snow production system in which snow is produced in external towers. The basic idea of the external snow production towers is to keep the temperature of the hall constant without the need for a colder temperature for snow production. The new system is designed with four external towers, each with one lance (mass flow water 0.5 l/s). Figure 9 shows a sketch of "SNØ" with the external snow towers in red. The snow production towers are designed with a height of 10 m and a diameter of 5 m.

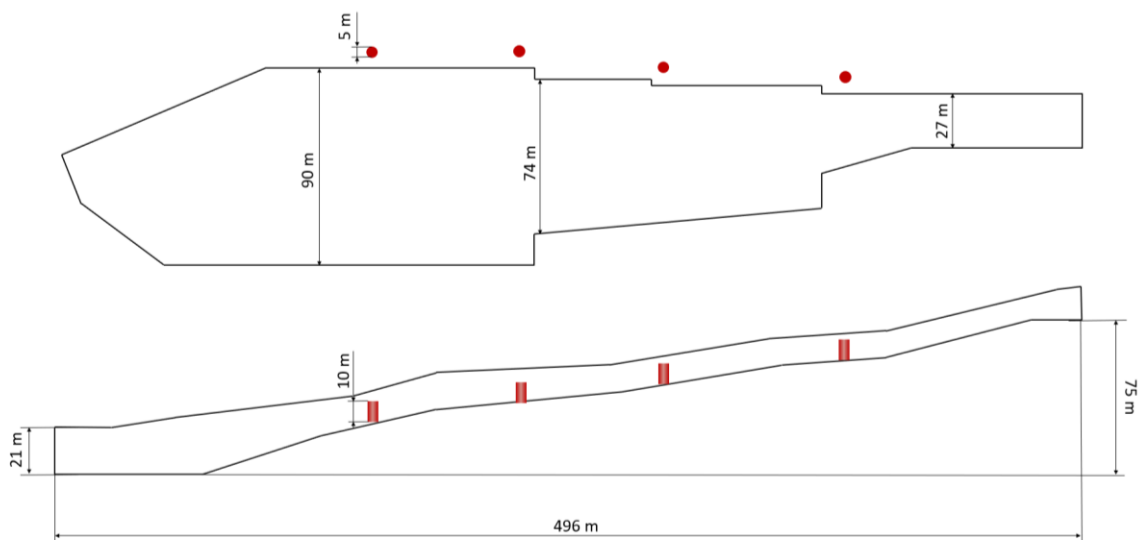


Figure 9: Sketch of the hall with the external snow production towers (red)

The production hall must be designed so that the drop freezes until it hits the ground. In chapter 3.1 the freezing time of the droplets will be calculated. From the calculation follows a freezing time of 20 s, with a typical droplet size of $400\text{ }\mu\text{m}$ and an air temperature of $-10\text{ }^{\circ}\text{C}$. In (Chen and Kevorkian 1971) the velocity of a droplet with a diameter of $700\text{ }\mu\text{m}$ was given with 3 m/s . From a freezing time of 20 s and an approximate speed of 3 m/s of the droplet, the tower would have to be 60 m high. In order to achieve a lower tower height, there must be an air

countercurrent which reduces the fall velocity of the droplets. A sketch of a production tower is shown in Figure 10.

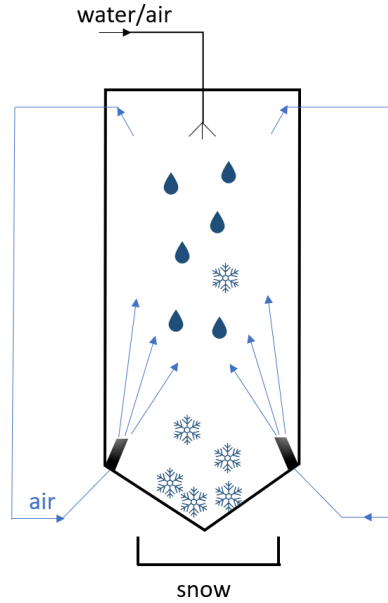


Figure 10: Sketch of production tower with air flow

3.1 Calculation of the droplet freezing time

To determine the dimensions of the external snow production site, the freezing time of a droplet must first be evaluated. To calculate the droplet freezing time the Excel tool of (Tolstorebrov 2021) was used. The calculation is based on the method of (Pham 1995). In (Akhtar et al. 2020), the heat transfer coefficients for three cases were evaluated for the different freezing stages. The heat transfer coefficient of the case with the highest free-stream velocity (0.54 m/s) was selected for the following freezing time calculation. The heat transfer coefficient incorporated the forced convection, evaporation, sublimation, radiation, and the heat losses due to the thermocouple, which was used for the measurements. The heat transfer coefficient was calculated as the mean value from the values of the different freezing stages (liquid supercooling, equilibrium freezing, solid subcooling). This results in a heat transfer coefficient of 156 W/(m² K). The thermophysical properties of water and ice are also taken from (Akhtar et al. 2020), see Table 7. The used parameter for the calculation are given by Table 3.

It should be noted here that the choice of this HTC is subject to greater uncertainties. Because the actual velocity of the droplet is higher than 0.54 m/s. In (Chen and Kevorkian 1971) the velocity of a droplet with a diameter of 700 μm was given with 3 m/s. The higher velocity also results in a higher HTC. Also, the formation of the average is not particularly precise but an

approximation. This approximation was made because no information about the times of the different freezing stages could be found.

Table 3: Parameter freezing time calculation

Initial water temperature	3 °C
Heat transfer coefficient	156 W/m ² K
Final droplet center temperature	-14 °C
Droplet diameter	100/400/700 μm
Droplet shape	Sphere

The results of the freezing time calculation are shown in Figure 11. According to the calculation, the freezing time for a droplet with a diameter of 400 μm is 20 s, when the air temperature is – 10°C.

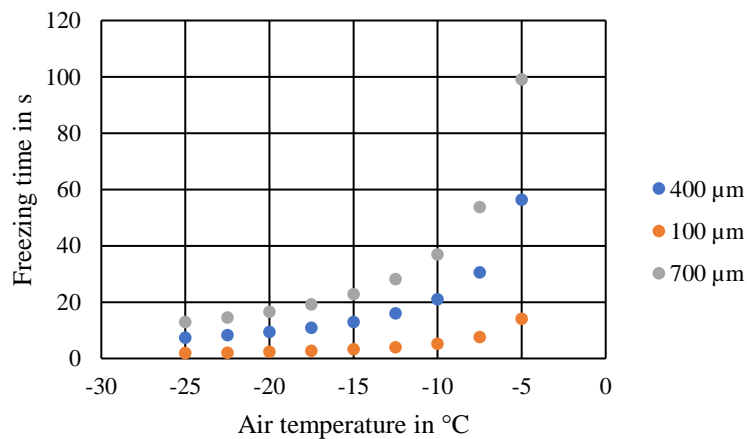


Figure 11: Freezing time as a function of the air temperature

In (Liao and C. 1989), the function for a typical droplet size distribution was plotted for the mean diameter between 200 and 400 μ, see Figure 12. It is difficult to predict the droplet size distribution. It depends on the nozzle geometry, the water and air pressure, the viscosity, and the surface tension. Further investigation is necessary to get the droplet size distribution on the specific application. In the product brochures of the manufacturers TechnoAlpin, Bächler Top Track AG or DemacLenko, no information on particle diameters was given (Techno Alpin 2021b; Bächler 2021; DemacLenko 2021).

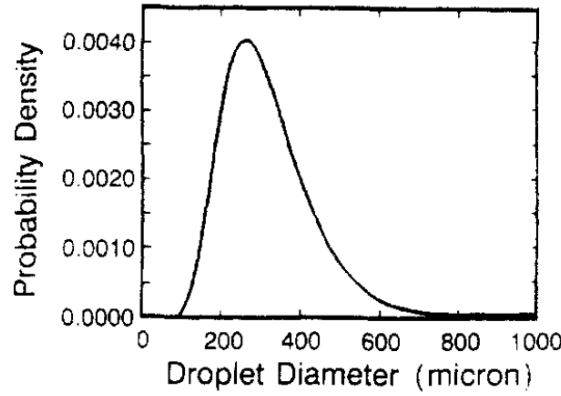


Figure 12: Typical droplet size distribution. (Liao and C. 1989)

Below are some literature results for the freezing time. According to (Chen and Kevorkian 1971), the freezing time is less than 15 s for droplets with a size between 200 and 700 μm under typical snow-making conditions. The terminal velocity of a falling droplet with a size of 100 μm is about 0.3 m/s, with a size of 700 μm it is about 3 m/s (Chen and Kevorkian 1971). From this follows a required height of 4.5 m or 45 m. In (Olefs et al. 2009) the traveling time of an artificially produced snow through the air is given with 10 to 15 s. If these results are compared with the calculated freezing time, it can be assumed that the actual freezing time may be shorter than calculated.

3.2 Humidity in the production towers

In order to develop a defrosting strategy, it is important to know how fast the humidity rises in the production tower. In the following the first step to estimate the humidity was made. To calculate the moisture gain during the snow production, the evaporation on the surface of a single droplet was calculated and then the moisture gain for all the droplets can be derived from it. The mass loss depends on the mass transfer coefficient, the drop surface and the partial pressures on the surface and in the ambient air, see equation (1). (Müller et al. 2015)

$$\dot{m} = -k_A \cdot A \cdot (\rho_{surf} - \rho_{air}) \quad (1)$$

The material properties needed for the calculation are given in Table 4. The thermal properties for the air are given for a temperature of -10 °C. The droplet is considered a liquid, so the density is for water at 0°C and the diffusion coefficient is from water to air.

Table 4: Thermal properties

Property		Value	Reference
Dynamic viscosity air (-10 °C)	η_{air}	$16.714 \cdot 10^{-7} \text{ m}^2/\text{s}$	(Kleiber and Joh 2021)
Kinematic viscosity air (-10°C)	ν_{air}	$126.2 \cdot 10^{-7} \text{ m}^2/\text{s}$	(Kleiber and Joh 2021)
Density air (-10°C)	ρ_{air}	1 3245 kg/m^3	(Kleiber and Joh 2021)
Density drop (0°C)	ρ_{drop}	999 kg/m^3	(Kleiber and Joh 2021)
Saturated vapor pressure (-10°C)	p_{sat}	260 Pa	(Zürcher and Frank 2018)
Diffusion coefficient water to air 0°C	$D_{0^\circ\text{C}}$	$23.0 \cdot 10^{-6} \text{ m}^2/\text{s}$	(Christen 2010)

The diffusion coefficient from water to air is temperature dependent. The conversion to a temperature of -10 °C is done with equation (2). (Christen 2010)

$$D_{-10^\circ\text{C}} = D_{20^\circ\text{C}} \frac{p_{0^\circ\text{C}}}{p_{-10^\circ\text{C}}} \cdot \left(\frac{T_{-10^\circ\text{C}}}{T_{0^\circ\text{C}}} \right)^{1.18} \quad (2)$$

To calculate the mass transfer coefficient, the Sherwood number must first be determined. For a spheric particle the Sherwood number is calculated by equation (3). This equation is valid for a Reynolds number between 0.1 and 10^4 and a Schmidt number between 0.6 and 10^4 . (Christen 2010)

$$Sh_{laminar} = 0.664 Re^{1/2} Sc^{1/3} \quad (3)$$

The Reynolds number and the Schmidt number are calculated by formula (4) and (5) (Christen 2010).

$$Sc = \frac{\nu_{air}}{D_{-10^\circ\text{C}}} \quad (4)$$

$$Re = \frac{\rho_{air} \cdot \nu_{drop} \cdot d}{\eta_{air}} \quad (5)$$

To get the mass transfer coefficient equation (4) is substituted in equation (6). After that, it is solved for the mass transfer coefficient. The mass transfer coefficient is given as a function of the diameter in equation (10).

$$Sh = \frac{k_A d}{D_{H2O/air}} \quad (6)$$

$$k_A = \frac{D_{H2O/air}}{d} \cdot 0.664 Re^{1/2} Sc^{1/3} \quad (7)$$

$$k_A = \frac{D_{-10}}{d} \cdot 0.664 \left(\frac{\rho_{air} \cdot v_{drop} \cdot d}{\eta_{air}} \right)^{1/2} \left(\frac{v_{air}}{D_{H2O/air}} \right)^{1/3} \quad (8)$$

$$k_A = d^{-0.5} \cdot D_{-10} \cdot 0.664 \left(\frac{\rho_{air} \cdot v_{drop}}{\eta_{air}} \right)^{1/2} \left(\frac{v_{air}}{D_{H2O/air}} \right)^{1/3} \quad (9)$$

$$k_A = d^{-0.5} \cdot C \quad (10)$$

$$C = D_{-10} \cdot 0.664 \left(\frac{\rho_{air} \cdot v_{drop}}{\eta_{air}} \right)^{1/2} \left(\frac{v_{air}}{D_{H2O/air}} \right)^{1/3} \quad (11)$$

The mass of the drop as a function of the diameter is given in equation (12). Then it is derived after the time, see equation (13).

$$m_{drop}(d) = \frac{d^3 \cdot \pi}{6} \cdot \rho_{drop} \quad (12)$$

$$\frac{dm_{drop}}{dt} = \frac{d^2 \cdot \pi}{2} \cdot \rho_{drop} \frac{dd}{dt} \quad (13)$$

Now equation (13) can be substituted in equation (1).

$$\frac{d^2 \cdot \pi}{2} \cdot \rho_{drop} \frac{dd}{dt} = -k_A \cdot (\rho_{surf} - \rho_{air}) \cdot d^2 \pi \quad (14)$$

$$\frac{1}{2} \cdot \rho_{drop} \frac{dd}{dt} = -d^{-0.5} \cdot C \cdot (\rho_{surf} - \rho_{air}) \quad (15)$$

$$d^{0.5} dd = -\frac{2C}{\rho_{drop}} \cdot (\rho_{surf} - \rho_{air}) dt \quad \Big| \int \quad (16)$$

$$\frac{2}{3} d^{3/2} = -\frac{2C}{\rho_{drop}} \cdot (\rho_{surf} - \rho_{air}) \cdot t + c_1 \quad (17)$$

$$d(t) = -\left(\frac{3C}{\rho_{drop}} (\rho_{surf} - \rho_{air}) \cdot t \right)^{\frac{2}{3}} + c_2 \quad (18)$$

For c_2 the initial diameter of the drop is used. A saturated state is assumed for the surface of the drop. To be able to use the saturated vapor pressure, equation (19) was used for the surface density. (Müller et al. 2015)

$$\rho_{surf} = \rho_{sat} = \frac{p_{sat} \cdot M_{H2O}}{T \cdot R} \quad (19)$$

The vapor pressure on the surface is the saturated vapor pressure over ice at the temperature of the room. For -10 °C it has a value of 260 Pa (Zürcher and Frank 2018). The vapor pressure of the ambient air can be calculated from the relative humidity, see equation (20) and then be used to calculate the density.

$$p_{air} = \varphi \cdot p_{sat} \quad (20)$$

$$\rho_{air} = \frac{p_{air} \cdot M_{H2O}}{T \cdot R} \quad (21)$$

Now the constant C from equation (11) and the densities (19) and (21) can be substituted in equation (18). Equation (22) follows from this. It can be used for further calculation of the moisture gain in the production towers.

$$d(t) = - \left(\frac{3D_{H2O/air} \cdot 0.664 \left(\frac{\rho_{air} \cdot v_{drop}}{\eta_{air}} \right)^{1/2} \left(\frac{v_{air}}{D_{H2O/air}} \right)^{1/3}}{\rho_{drop}} \left(\frac{p_{sat} \cdot M_{H2O}}{T_{surf} \cdot R} - \frac{p_{air} \cdot M_{H2O}}{T_{air} \cdot R} \right) \cdot t \right)^{\frac{2}{3}} + c_2 \quad (22)$$

4 Energy analysis

In the following, the amount of energy that can be saved by keeping the temperature in the hall constant is calculated. The energy savings are the energy that must be expended to cool the hall to the lower temperature and in the additional transmission heat losses. Equation (23) gives the energy to cool the air in the hall down to the lower temperature.

$$Q_{cool} = m_{air}(h_{i,highTemp} - h_{i,low,Temp}) \quad (23)$$

The enthalpy for the air can be calculated with equation (24). (Doering et al. 2016)

$$h_{1+x} = \bar{c}_{p,A} \cdot t + x(\Delta h_v + \bar{c}_{p,V} \cdot t) \quad (24)$$

Equation (25) gives the mean specific heat capacity for air and for vapor. The specific heat capacities used for this equation can be found in Table 8 in the appendix.

$$\bar{c}_p|_{t_0}^{t_2} = \frac{c_p|_{t_0}^{t_2}(t_2 - t_0) - c_p|_{t_0}^{t_1}(t_1 - t_0)}{t_2 - t_1} \quad (25)$$

The mass of the humid air is calculated from the ideal gas law and the Dalton's law of partial pressures. (Doering et al. 2016)

$$m_{air} = \frac{(p - \varphi \cdot p_{v,sat}) \cdot V_{hall}}{R_{air}T} + \frac{(\varphi \cdot p_{v,sat}) \cdot V_{hall}}{R_{vapor}T} \quad (26)$$

The transmission losses are calculated with the equation (27) and (28). For the outdoor temperatures the weather data from the meteorological station of Lillestrøm were used (Norwegian Meteorological Institute 2021). The temperatures refer to the year 2020. Due to missing data from June 3 to September 7, data from 2021 was used for this period. As mentioned before, the temperature of "SNØ" is lowered from Sunday 6 pm to Monday 3 pm, thus for 21 hours. To simplify the calculation the average day temperature is used. The outdoor temperature used in equation (28) is the average of the values of all Sundays in 2020. The U-value for the walls is 0.22 W/m²K and for the ceiling 0.18 W/m²K (Klingenberg 2021). The area of the ceiling is assumed to be the same as the snow surface, i.e. 32 000 m² (Klingenberg 2021). The external walls have an area of about 2 780 m². The southwestern wall, with an area of approximately 1 200 m² is adjacent to the adjoining building complex. To consider the transmission to the adjacent building complex, it is calculated separately. Since no more precise information is available, the U-value is assumed to be 0.22 W/m²K and the temperature in the adjacent building is assumed to be constant at 20 °C. The information on ceilings and wall areas

was calculated from technical drawings (Klingenberg 2021). However, due to the complex geometry, these are only approximate values.

$$Q_{trans} = Q_{trans,wall,ext} + Q_{trans,wall,build} + Q_{trans,ceiling} \quad (27)$$

$$Q_{trans} = UA\Delta T \quad (28)$$

The additional transmission losses when the internal temperature is lowered can be calculated using equation (29).

$$Q_{trans,add} = Q_{trans,lowTemp} - Q_{trans,highTemp} \quad (29)$$

The saved transmission energy and the energy for cooling give the total saved energy, see equation (30).

$$Q_{add} = Q_{trans,add} - Q_{cool} \quad (30)$$

The following results refer to an air volume in the hall of 470 000 m³ and a humidity of 80 %. From equation (23) follows that 439 kWh are at least needed to cool down the air in the hall by 1 K. This means that decreasing the temperature in the hall from -5 °C to -10 °C needs at least 2 199 kWh. In Figure 13 this is also shown for other temperatures. The additional transmission losses compared to -5 °C are also given. The transmission losses are based on the calculated average outdoor temperature of 8.3 °C in 2020.

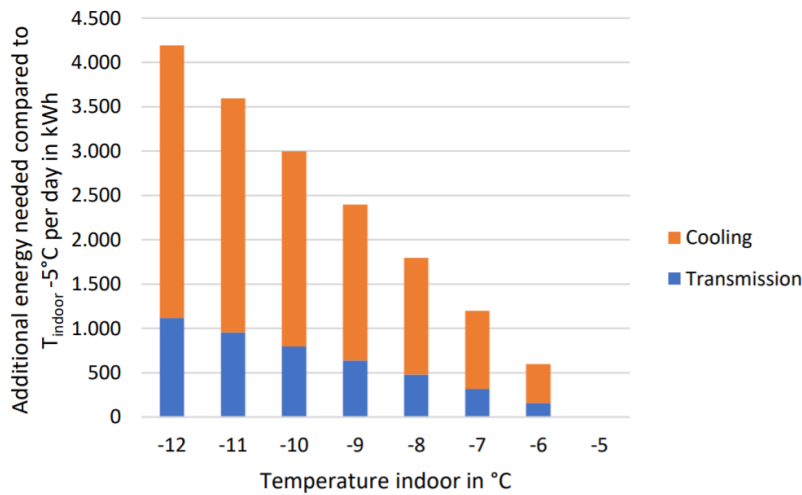


Figure 13: Additional energy needed compared to an indoor temperature of - 5 °C with lower temperature. Considering additional transmission losses for an average outdoor temperature of 8.3 °C. E_{cool} for starting temperature of - 5 °C.

In Figure 14 the energy demand for the different outdoor temperatures is shown. The snow production is not considered here.

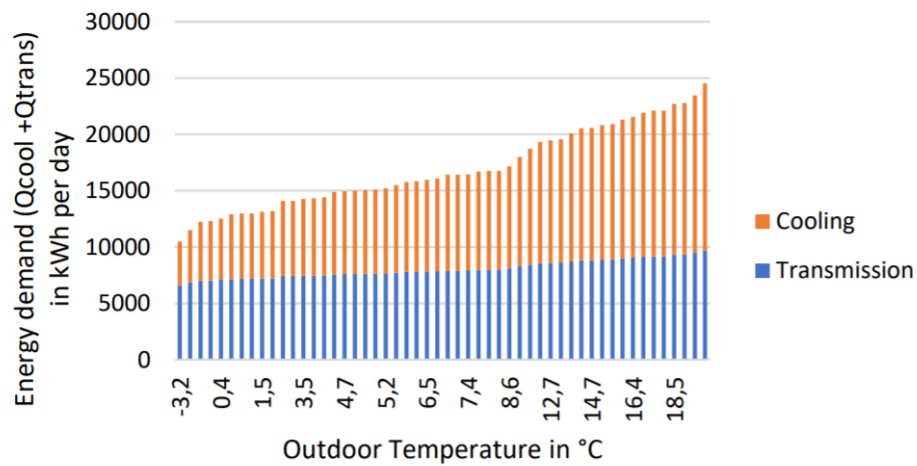


Figure 14: Energy demand ($Q_{cool}+Q_{trans}$) for an indoor temperature of $-10\text{ }^{\circ}\text{C}$

The designed refrigeration system based on CO_2 as a refrigerant is shown in Figure 15. The system is designed as a central refrigeration system with medium temperature evaporators for the hall and low temperature evaporators for the snow production towers.

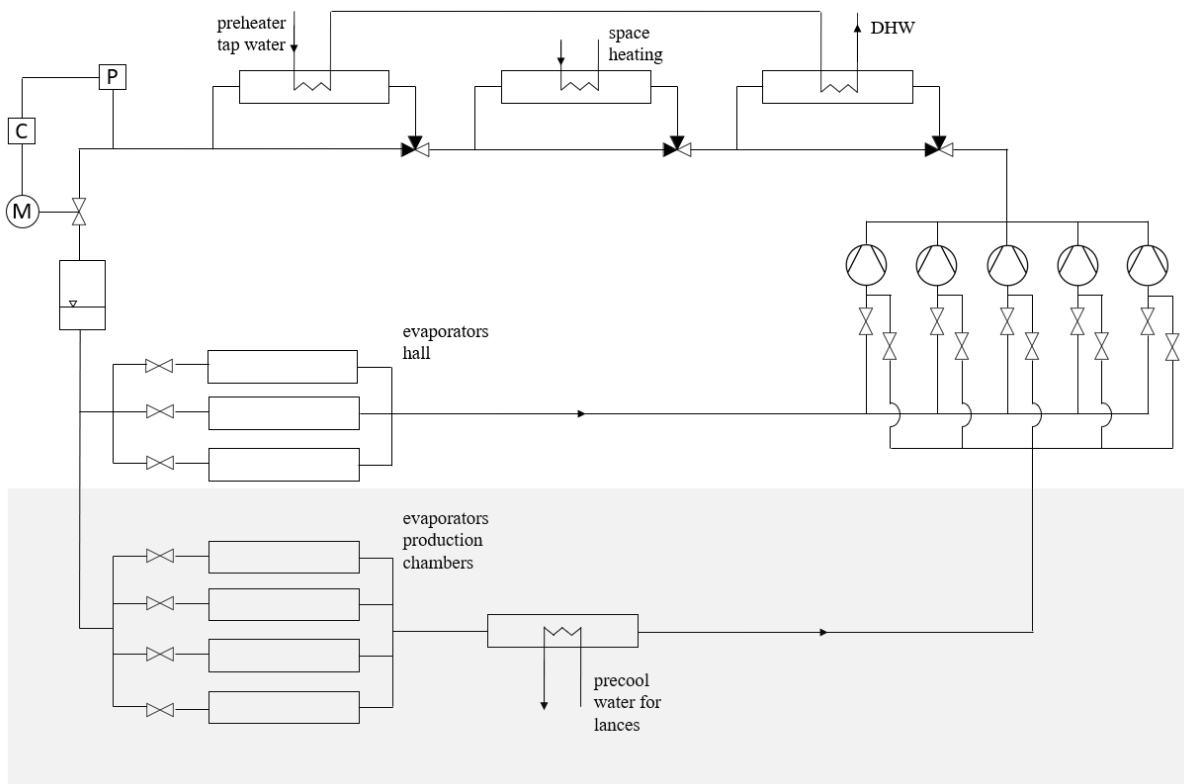


Figure 15: Refrigeration system

Basically, it is the current refrigeration system extended by the evaporators for the snow production towers. After the evaporators for the snow production towers a superheater is used to precool the water for the lances. A heat recovery system is used to provide domestic hot water and space heat. The third gas cooler (left one) preheats the tap water, which is then heated up to 70 °C in the first gas cooler (right one). The second gas cooler provides heat at a medium temperature for space heat. When no space heat is required, it can be released into the ambient air.

The temperature of the tap water entering the third gas cooler is assumed to be 5 to 10 °C. Based on this, the temperature of the refrigerant after the gas coolers is set at 15°C. The entry temperature of CO₂ into the evaporators of the hall is set at - 10 °C. For the evaporators of the snow production towers the entry temperature is set at – 20 °C. The isentropic efficiency of the compressors is assumed to be 0.85.

For the cooling load for the hall only the transmission losses are regarded, see equation (31). The transmission load is calculated analogously to equation (27), with the average ambient temperature 8,2 °C and an indoor temperature of -10 °C. The infiltration load is neglected, because no precise information is available. The hall envelope has a passive house standard, but greater infiltration losses are to be expected via the access gate for the snow groomer.

$$Q_{hall} = Q_{trans,hall} \quad (31)$$

To calculate the cooling load (equation (32)) for the snowmaking towers, some assumptions must be made. The snow production system consists of four towers, each with one lance. One lance has a water mass flow of 0.5 l/s. A tower is designed with a height of 10 m and a diameter of 5 m. The U-value for the wall and the ceiling is assumed to be 0.22 W/m²K. The transmission load is calculated analogously to equation (28), with the average ambient temperature and a temperature of -15 °C in the tower. The load for the snow production is composed of the load due to the cooling and freezing of the droplets, see equation (33) to (35). The energy consumption of the fan, which generates the air counterflow in the production tower, is neglected here, because the required air mass flow has not been calculated in this work.

$$Q_{chambers} = Q_{trans,chambers} + Q_{snow} \quad (32)$$

$$Q_{snow} = Q_{sensible} + Q_{latent} \quad (33)$$

$$Q_{sensible} = \dot{m}_{water} \cdot c_{p,w} \cdot (T_{3^{\circ}C} - T_{0^{\circ}C}) + \dot{m}_{water} \cdot c_{p,ice} \cdot (T_{0^{\circ}C} - T_{-15^{\circ}C}) \quad (34)$$

$$Q_{latent} = \dot{m}_{water} \cdot h_{fusion} \quad (35)$$

At present, it is difficult to estimate infiltration losses because they depend strongly on the design of the tower and their operation. For this reason, infiltration losses are neglected. The same applies to the losses due to defrosting.

Since snow production is expected to be only once a week, there is the need to cool down the tower. The energy needed to do this, can be calculated with equation (36). The mass of the air is calculated with equation (26) and an assumed relative humidity of 80 %. For the calculation of the enthalpies equation (24) is used. This energy must be applied before the snow production can start.

$$Q_{cool,towers} = m_{air}(h_{ambient,temp} - h_{-15^{\circ}C}) \quad (36)$$

Table 5 shows the cooling demands for the case where only the hall is cooled and for the case of snow production, where the cooling of the hall is not considered.

Table 5: Cooling demands

Q_{hall}	301 kW
Q_{towers}	756 kW
$Q_{trans,towers}$	3.1 kW
Q_{snow}	753.2 kW
$Q_{cool,towers}$	3.3 kWh

For the case where only the hall is cooled, the COP for cooling is calculated with equation (37). Equation (38) gives the COP for the heating in the winter case, when space heating is needed.

$$COP_{cooling,hall} = \frac{Q_{hall}}{W_{comp}} \quad (37)$$

$$COP_{heating,hall} = \frac{Q_{gascooler}}{W_{comp}} \quad (38)$$

In the case where only the snow production towers are cooled, the COP for cooling can be calculated by equation (39). When the waste heat can be used, the COP for heating is given by equation (40).

$$COP_{cooling,tower} = \frac{Q_{chambers} + Q_{superheat}}{W_{comp}} \quad (39)$$

$$COP_{heating,tower} = \frac{Q_{gascooler}}{W_{comp}} \quad (40)$$

The resulting values for the refrigeration system are given in Table 6. The refrigeration process is also shown in the pressure-enthalpy diagram in Figure 16. The pressure and enthalpy of each point is given in Table 9 and Table 10 in the appendix.

Table 6: Results calculation refrigeration system

	System hall	System tower
\dot{m}_{CO_2}	1.6 kg/s	3.8 kg/s
W_{comp}	90 kW	333 kW
$Q_{gascooler}$	391 kW	1 148 kW
Q_{evap}	301 kW	756 kW
$Q_{superheat}$	-	59 kW
$COP_{cooling}$	3.4	2.5
$COP_{heating}$	4.3	3.5

The saved cooling demand when using the external production towers compared to snow production in the hall is calculated according to equation (41).

$$Q_{saved} = Q_{cool,hall} + Q_{trans,add} - Q_{coll,towers} - Q_{trans,towers} \quad (41)$$

$$Q_{saved} = 2\,199\,kWh + 796\,kWh - 3\,kWh - 74\,kWh = 2\,918\,kWh$$

This 2 918 kWh are saved during 24 hours of snow production, when the snow is produced in the external towers. This is equivalent to 864 kWh of electricity if the CO₂-based refrigeration system described earlier is used. Assuming 52 day of snow production per year, this results in 44 928 kWh of electricity per year. According to (Klingenberg 2021) the energy consumption of the hall is about 500 000 kWh per month, thus 6 000 000 kWh per year. It follows, that the energy savings when using external production towers is equivalent to 0.7 % of the total energy consumption.

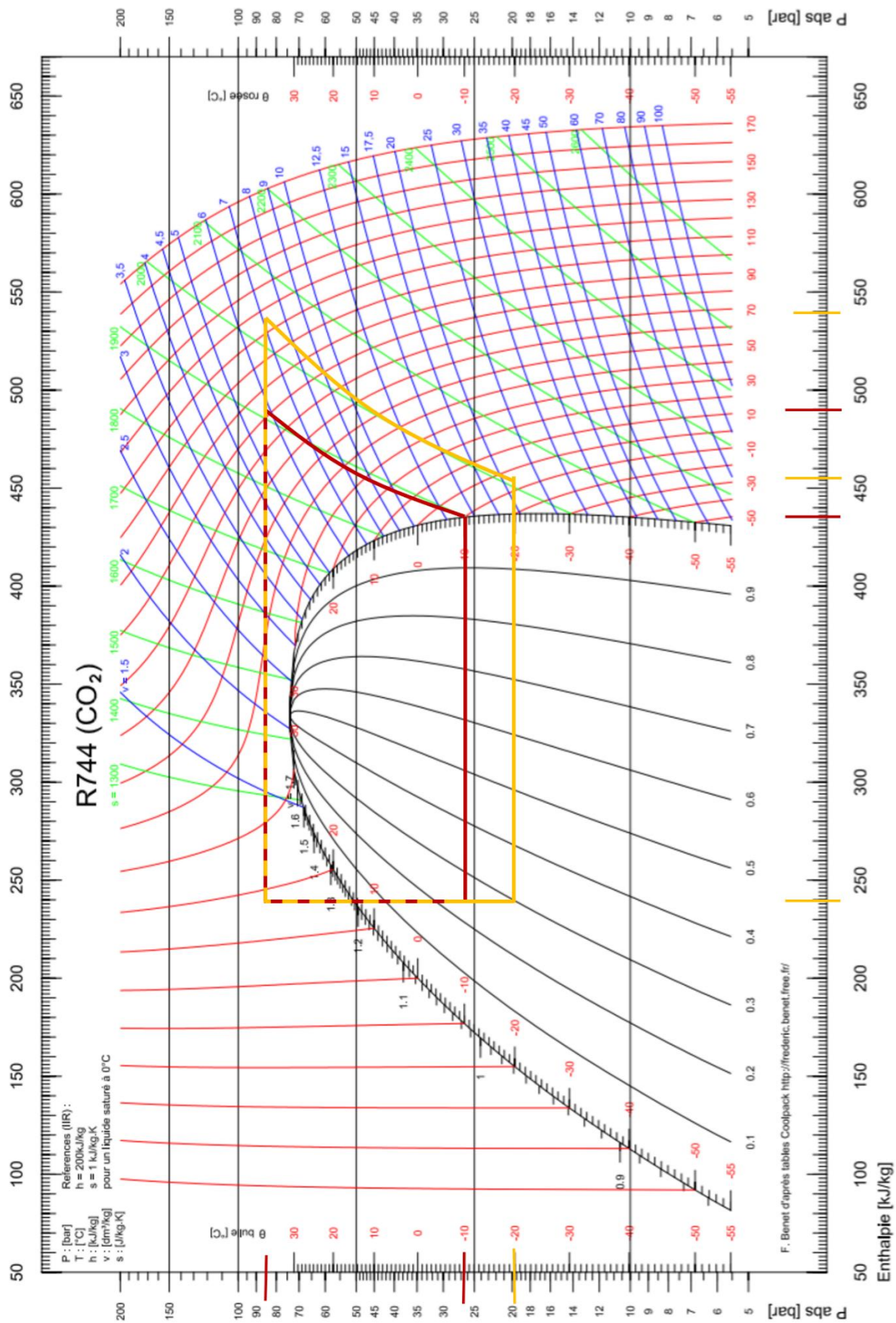


Figure 16: Pressure-Enthalpy diagram CO₂

5 Defrosting systems for evaporators

A good overview of research on defrosting methods is provided by (Badri et al. 2021) and (Amer and Wang 2017). Defrosting methods can be divided in active, passive and system methods. Active methods are electrohydraulic defrosting, oscillation, or ultrasonic vibration. Surface modification that reduces or delay frost formation are classified as passive methods. The most common methods are the system methods, such as process reversal, hot gas bypass, electric heaters, desiccant dehumidifiers. (Amer and Wang 2017)

Surface modification

In (Amer and Wang 2017), the effect of surface modifications such as different structure or coatings on the frost formation and defrosting are described. A micro-grooved surface improved the drainage of the frost melt, which reduces the energy required for defrosting (Amer and Wang 2017). A slippery surface also has good drainage properties, but at low temperatures this advantage becomes negligible (Badri et al. 2021). Superhydrophobic surfaces showed a later initialization of frosting, a shorter frost melting time and less retained water on the surface compared to a bare surface (Amer and Wang 2017).

Electrohydraulic defrosting

For the electro-hydrodynamic defrosting method, a high voltage electric field is employed to the airflow. The frost layer is more fragile when the electric field is applied. This results in a shorter defrosting time, but compared to modified surfaces, the effect is not as good. In addition, the effectiveness of this method is lower at high velocities and forced convection. (Amer and Wang 2017)

Ultrasonic vibration

Ultrasonic vibration can cause the collapse of frost crystals. Another mechanism is that the deposition of water vapor on the surface is suppressed because the concentration gradient profile of the water vapor on the surface is interrupted. These are the effects why ultrasonic vibration helps to delay the frost growth and shorten the defrosting time. The literature reviewed in (Amer and Wang 2017) on defrosting with ultrasonic vibration showed good results, but more research is needed, especially with regard to specific applications. (Amer and Wang 2017)

Electric resistive heaters

The electric resistive heaters are embedded in the heat exchangers. They are mainly used for low capacity applications because of their high energy consumption. In (Amer and Wang 2017), the comparison between reverse cycle defrosting and electric heating showed that the energy consumption of electric heating was 27% higher.

Reverse cycle defrosting

For reverse cycle defrosting, the direction of the refrigerant flow is changed. A four-way valve is used for that. In (Wang et al. 2020), it is stated that reverse cycle defrosting cannot be used for transcritical CO₂ applications, because there are no suitable four-way valves for the high pressure conditions. The hot gas defrosting is seen as a more feasible option. (Ye et al. 2021) compared the reverse cycle and the hot gas bypass defrosting for a transcritical CO₂ heat pump water heater. To get around the four-way valve problem, two three-way valves were used for the experimental setup. The study showed that the reverse cycle could be a promising solution, as it has a significantly higher energy performance compared to the hot gas bypass.

Hot gas bypass

In (Hu et al. 2015), hot gas defrosting is studied for a transcritical CO₂ heat pump system, it was concluded that hot gas defrosting is more beneficial compared to other methods. The hot gas bypass method uses the superheated refrigerant from the compressor to defrost the evaporator. The refrigerant bypass the gas cooler and the expansion device and goes directly to the evaporator. (Amer and Wang 2017)

In (Wang et al. 2020) the hot gas bypass defrosting for an transcritical CO₂ heat pump was investigated. In Figure 17 the schematic of the transcritical CO₂ heat pump during the hot gas bypass defrost is shown. In the defrosting mode the defrosting solenoid valve (DSV) is open. Then the compressed CO₂ is throttled by the expansion device and defrosts the evaporator. The defrosting efficiency was evaluated to be between 41 % to 51 %, depending on the ambient temperature.

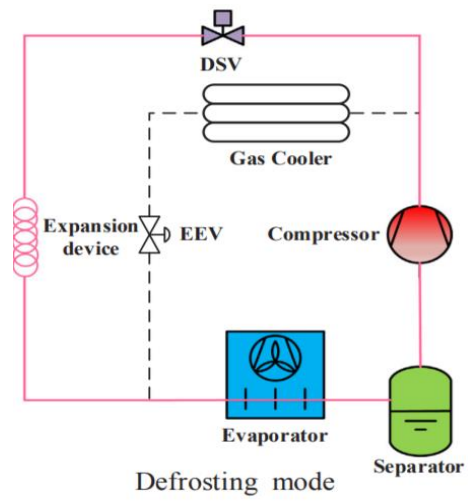


Figure 17: Schematic of hot gas bypass defrosting of an transcritical CO₂ heat pump. (Wang et al. 2020)

6 Conclusions and suggestions for further work

6.1 Conclusion

The literature research showed that despite an increasing number of indoor ski facilities, the literature on this subject is still limited, especially with regard to the energy aspects. The limited amount of literature on artificial snow and indoor ski facilities makes it clear that more research is needed in this area.

This work showed that the energy consumption can be reduced when the snow is produced in external production towers rather than indoors. The developed snow production system consists of four production towers with a centralized CO₂ based refrigeration system. The calculation of the freezing time for different sizes and air temperatures showed that a typical droplet with a size of 400 µm needs 20 s to freeze, when the air temperature is – 10°C. This concludes that the production towers have to be designed with an air counterflow to achieve the required freezing time. With the new snowmaking system, the energy consumption can be reduced by 44 928 kWh of electricity per year. This is about 0.7 % of the total energy consumption of the reference system "SNØ". A formula for the evaporation from the surface of a droplet has been derived. This formula will help to calculate the rise of humidity in the production towers during the snow production. It is important to know how much and fast the humidity is increasing in order to develop a defrost strategy for the evaporators. An overview of defrosting methods was given in the last part of this thesis.

6.2 Suggestions for further work

Based on this work, the following aspects are proposed for further work:

- based on the formula for the evaporation during the freezing process of a drop, a formula for calculating the moisture increase should be developed
- the refrigeration system which includes the evaporators for the snow production towers should be planned in detail
- calculation of the air mass flow which is needed to achieve the required falling time for the snow production
- the energy balance of the production towers should be extended by the energy consumption of the fan for the air flow and the heat gain due to defrosting
- design of the defrosting system for the evaporators and development of a defrosting strategy

7 References

- A. Koptug, J. Aström, L. Ananiev (2006). How to make perfect snow. Mid-Sweden University.
- Afry (2021). Arenas- Prioritet Serneke Arena. Available online at <https://afry.com/en/project/arenas-prioritet-serneke-arena> (accessed 9/16/2021).
- Akhtar, Saad/Xu, Minghan/Sasmito, Agnus (2020). Development and validation of a semi-analytical framework for droplet freezing with heterogeneous nucleation and non-linear interface kinetics. Montreal 2020.
- Amer, Mohammed/Wang, Chi-Chuan (2017). Review of defrosting methods. Taiwan 2017.
- Arnold Ofner, Christoph Pauly (2006). Pumps and valves for snow generation.
- Bächler (2021). SnoTek Tridudsa. Available online at https://www.bachler.ch/media/archive1/produkte/BTT_FactSheet_SnoTekTRIDUSA_EN.pdf (accessed 10/20/2021).
- Badri, Deyae/Toublac, Cyril/Rouaud, Olivier/Havet, Michel (2021). Review on frosting, defrosting and frost management techniques in industrial food freezers. Nantes, France 2021.
- Cardillo, Lucio/Corsini, Alessandro/Delibra, Giovanni (2015). Axial flow fan design Experience for a project based turbomachinery class. Montréal.
- Chen, Jamin/Kevorkian, Victor (1971). Heat and Mass Transfer in Making Artificial Snow.
- Christen, Daniel S. (2010). Praxiswissen der chemischen Verfahrenstechnik. Handbuch für Chemiker und Verfahreningenieure. 2nd ed. Berlin, Heidelberg, Springer Berlin Heidelberg.
- DemacLenko (2021). EOS 1. Available online at <https://www.demaclenko.com/en/lances/eos-1/43-326311.html> (accessed 10/20/2021).
- Doering, Ernst/Schedwill, Herbert/Dehli, Martin (2016). Feuchte Luft. In: Ernst Doering/Herbert Schedwill/Martin Dehli (Eds.). Grundlagen der technischen Thermodynamik. Lehrbuch für Studierende der Ingenieurwissenschaften. 8th ed. Wiesbaden, Springer Vieweg, 407–428.

- Eurrer, Thomas (2021). Schneilanze EOS. Available online at <https://www.simagazin.com/si-magazin/schneilanze-eos-effizienzwunder-der-beschneigung/> (accessed 10/1/2021).
- Fanasiutkia, Aleksandra (2015). The organisation of air exchange of ski tunnel. Bachelor Thesis. Lappeenranta, Saimaa University of Applied Sciences.
- Fredheim, Sofie (2019). Energy systems for an artificial cross-country skiing tunnel. Master thesis. Gothenburg, Chalmers University of Technology.
- Fröjd, Henrik (2014). Energieffektiv produktion och lagring av snö för skidtunnel. Luleå, tekniska universitet.
- Hu, Bin/Yang, Dongfang/Cao, Feng/Xing, Ziwen/Fei, Jiyu (2015). Hot gas defrosting method for air-source transcritical CO₂ heat pump systems. *Energy and Buildings* 86, 864–872. <https://doi.org/10.1016/j.enbuild.2014.10.059>.
- Kleiber, Michael/Joh, Ralph (2021). Erratum to: D1 Berechnungsmethoden für Stoffeigenschaften. Available online at https://link.springer.com/referenceworkentry/10.1007%2F978-3-642-19981-3_114 (accessed 11/17/2021).
- Klingenberg, Trym (2021). Personal communication (E-Mail) 2021.
- Liao, James/C., Kam (1989). Effect of ice nucleators on snow making and spray freezing. New York 1989.
- MidSweden365 (2021). Homepage. Available online at <https://midsweden365.se/om-oss/> (accessed 10/8/2021).
- Müller/Bernhard/Finkenrath/Matthias (2015). Formelsammlung Thermodynamik, Wärme- und Stoffübertragung und Strömungsmechanik: mit Stoffwertetabellen und -diagrammen.
- Norwegian Meteorological Institute (2021). Weather data 2020 Lillestrøm. Available online at <https://www.yr.no/en/statistics/table/1-73669/Norway/Viken/Lillestr%C3%B8m/Lillestr%C3%B8m?q=2020-08> (accessed 11/23/2021).
- Olefs, Marc/Fischer, Andrea/Lang, Josef (2009). Boundary Conditions for Artificial Snow Production in the Austrian Alps. *Journal of Applied Meteorology and Climatology* 49, 1096–1113 2009.

- Pham, Q. T. (1995). Comparison of general purpose finite element methods for the stefan problem 1995.
- Singh, Vijay P./Singh, Pratap (2011). Encyclopedia of Snow, Ice and Glaciers. Netherlands.
- Sipilä, Kari/Rämä, Miika (2009). Integrated heating and cooling production in sport halls. Helsinki.
- Skoblickaya, Yulia/Sherement, Anastasia (2019). The architectural and planning organization of the closed complexes for winter sports. Journal of Environmental Management and Tourism 10 (5) 2019.
- Techno Alpin (2021). Indoor snow. Available online at <https://indoor.technoalpin.com/downloads.html> (accessed 9/30/2021).
- Techno Alpin (2021b). TL Serie. Available online at https://www.technoalpin.com/fileadmin/user_upload/Pdf/TL_Serie_Prospekt_De.pdf (accessed 10/20/2021).
- Tolstorebrov, Ignat (2021). E-mail correspondence. Freezing Time Calculation 2021.
- Trædal, Stian (2017). Temperature independent snow production. SINTEF Energi AS. 978-82-14-06596-1. Available online at <https://sintef.brage.unit.no/sintef-xmlui/handle/11250/2627058>.
- Vagle, Bernhard Haver (2016). Utilization of surplus heat from snow producing machines. Trondheim, NTNU.
- Wang, Yikai/Ye, Zuliang/Song, Yulong/Yin, Xiang/Cao, Feng (2020). Experimental investigation on the hot gas bypass defrosting in air source transcritical CO₂ heat pump water heater. Applied Thermal Engineering 178, 115571. <https://doi.org/10.1016/j.applthermaleng.2020.115571>.
- Website Skidome Göteborg (2021). Skidome. Available online at <https://www.skidome.ski/> (accessed 9/14/2021).
- Website Skihall Oberhof (2021). Data and Facts. Available online at <https://www.oberhof-skisporthalle.de/skihalle/daten-und-fakten> (accessed 9/16/2021).
- Website Thüringer Wintersportzentrum (2021). Lotto Thüringen Skisport-Halle. Available online at <https://www.wintersportzentrum-thueringen.de/skisport-halle/die-sportstaette> (accessed 9/16/2021).

Website Vesileppis. Vesileppis ski arena. Available online at <https://www.vesileppisliikuntapalvelut.fi/hiihtoareena>.

Website Vuokatti (2021). Ski Tunnel and the first snow track. Available online at <https://vuokattisport.fi/en/hiihtotunneli-firstsnowtrack/> (accessed 9/14/2021).

Xin Zhao, Bo Dong, Weizhong Li (2018). Analysis of the freezing process about a falling droplet using the lattice Boltzmann method. *International Journal of Numerical Methodes for Heat and Mass Transfer* 10.

Ye, Zuliang/Wang, Yikai/Yin, Xiang/Song, Yulong/Cao, Feng (2021). Comparison between reverse cycle and hot gas bypass defrosting methods in a transcritical CO₂ heat pump water heater. *Applied Thermal Engineering* 196, 117356. <https://doi.org/10.1016/j.applthermaleng.2021.117356>.

Zürcher, Christoph/Frank, Thomas (2018). *Bauphysik. Bau und Energie*. 5th ed. Zürich, vdf Hochschulverlag AG an der ETH Zürich.

Appendix

Table 7: Thermal properties water (Akhtar et al. 2020)

Specific heat (unfrozen)	4200 J/kgK
Thermal conductivity (unfrozen)	0.555 W/mK
Density (unfrozen)	1000 kg/m ³
Specific heat (frozen)	2100 J/kgK
Thermal conductivity (frozen)	2.22 W/mK
Density (frozen)	916 kg/m ³
Latent heat	334 000 J/kg

Table 8: Specific heat capacities dry air and vapor (Doering et al. 2016)

Temperature in °C	C _{p,A}	C _{p,V}
-20	1,0055	1,857
0	1,0056	1,858
20	1,0058	1,86
40	1,0062	1,863

Table 9: Refrigeration system hall (pressure, enthalpy)

Point	1	2is	2	3	4
pressure in bar	27	85	85	85	27
Enthalpy in kJ/kg	433	482	490	240	240

Table 10: Refrigeration system towers

(pressure, enthalpy)

Point	1	1 _{superheat}	2is	2	3	4
pressure in bar	20	20	85	85	85	20
Enthalpy in kJ/kg	439	455	529	542	240	240

